

# Harmonious Inter-decadal Changes of July–August Upper Tropospheric Temperature Across the North Atlantic, Eurasian Continent, and North Pacific

ZHOU Tianjun<sup>1</sup> (周天军) and ZHANG Jie<sup>1,2</sup> (张洁)

<sup>1</sup>*State Key Laboratory of Numerical Modeling for Atmospheric Sciences and Geophysical Fluid Dynamics, Institute of Atmospheric Physics, Chinese Academy of Sciences, Beijing 100029*

<sup>2</sup>*Graduate University of Chinese Academy of Sciences, Beijing 100049*

(Received 16 January 2009; revised 21 March 2009)

## ABSTRACT

The authors have developed an integral view of the inter-decadal variability of July–August (JA) tropospheric temperature across the entire subtropical Northern Hemisphere. Using reanalysis data and complementary balloon-borne measurements, the authors identify one major mode of variability for the period 1958–2001 which exhibits a significant cooling center over East Asia and warming centers over the North Atlantic and North Pacific. The cooling (warming) signals barotropically penetrate through the troposphere, with the strongest anomalies at 200–300 hPa. The amplitude of the cooling over East Asia is stronger than that of the warming over the North Atlantic (North Pacific) by a factor of 2 (3). This dominant mode exhibits a declining tendency for the entire period examined, particularly before 1980. After the mid-1980s, the tendency has leveled off. Variations of the harmonious change of JA upper tropospheric temperature represented by the principal component of Empirical Orthogonal Function analysis exhibit significant negative (positive) correlations with SST anomalies in the eastern tropical Pacific and the western tropical Indian Ocean (mid-latitude North Pacific). Possible mechanisms are discussed.

**Key words:** tropospheric temperature, inter-decadal variability, harmonious changes

**Citation:** Zhou, T. J., and J. Zhang, 2009: Harmonious inter-decadal changes of July–August upper tropospheric temperature across the North Atlantic, Eurasian continent, and North Pacific. *Adv. Atmos. Sci.*, **26**(4), 656–665, doi: 10.1007/s00376-009-9020-8.

---

## 1. Introduction

Temperature changes are one of the most obvious and easily measured changes in climate. Previous discussions of climate change have tended to focus on past and future changes in surface air temperature (e.g., Wang and Gong, 2000; Jones and Moberg, 2003; Zhou and Yu, 2006). Since most climate change processes occur in the troposphere, any assessment of climate change and variability should consider both the surface and the troposphere. Great efforts have been devoted to the investigation of tropospheric temperature change in recent years, and new analyses of balloon-borne and satellite measurements of lower- and mid-tropospheric temperature show warming rates that

are similar to those of the surface temperature record (Trenberth et al., 2007).

The tropospheric temperature variation exhibits regional features. For example, contrary to the warming trend elsewhere, a spring cooling trend extending from surface to tropopause is found across the subtropical Eurasia continent over the last half century (Yu and Zhou, 2004). Variations of tropospheric temperature over East Asia show distinctive features, partly due to the complex topography. A recent examination of the spring tropospheric temperature change over the eastern flank of the Tibetan Plateau revealed the contribution of the plateau to a cooling shift via continental stratiform cloud-climate feedback (Yu et al., 2004a; Li et al., 2005). The significance of the Ti-

---

Corresponding author: ZHOU Tianjun, zhoutj@lasg.iap.ac.cn

betan Plateau as an elevated heat source for the abrupt seasonal change and Asian monsoon onset has been discussed by many authors (e.g., Ye and Gao, 1979). Seasonal upper tropospheric warming over the eastern Tibetan Plateau has been suggested to be the primary cause of the reversals of the meridional temperature gradient associated with monsoon onset. Variations of tropospheric temperature over the plateau contribute to the South (East) Asian summer monsoon, via changes of the meridional (zonal) land-sea thermal contrast (Li and Yanai, 1996; Wu, 2005; Zhao et al., 2007).

East Asian climate has experienced an inter-decadal scale transition near the end of 1970s (Hu, 1997; Wang, 2001; Hu et al., 2003; Han and Wang, 2007). Associated with the inter-decadal climate transition, a strong tropospheric cooling trend is prominent over East Asia during July and August, which contributes to the tendency toward increased droughts in northern China and floods along the Yangtze River valley (often referred to as South China Flood and North China Drought) through changes to the East Asian atmospheric circulation (Yu et al., 2004b). This cooling trend has been verified recently by balloon-borne measurements (Duan, 2007; Yu and Zhou, 2007). A similar mechanism applies to the spring-time inter-decadal scale climate change over south-eastern China, which has been manifested as a tendency toward drought over the past half century (Xin et al., 2006). However, previous discussions only focused on East Asia and have ignored the fact that a warming trend is also evident over the mid-latitude North Atlantic and North Pacific accompanying the cooling over East Asia (c.f. Fig. 1 of Yu et al., 2004b). The present study aims to address the following questions: (1) Is the tropospheric temperature change over East Asia significantly related to temperature changes over the North Atlantic and North Pacific? (2) What is the dominant mode of the tropospheric temperature change across the North Atlantic, Eurasian continent, and North Pacific? Based on reanalysis data and complementary balloon-borne measurements, we show that the tropospheric temperature cooling over East Asia is a local manifestation of a major mode of variability for the period 1958–2001, which exhibits a significant cooling center over East Asia and warming centers over the North Atlantic and North Pacific. This dominant mode exhibits a declining tendency for the entire period examined. After the mid-1980s, however, this tendency has leveled off.

The rest of the paper is organized as follows. We first introduce the data and analysis methods in section 2. We then present the results in section 3. A discussion is given in section 4. Section 5 summarizes

the main findings.

## 2. Data and methods description

The data used in the present study consist of: (1) the European Centre for Medium-Range Weather Forecasts 40-Year Reanalysis (ERA-40) dataset from 1958 to 2001 (Uppala et al., 2005); (2) the Hadley Centre's radiosonde temperature product HadAT, which contains globally gridded radiosonde temperature anomalies from 1958 to present (Thorne et al., 2005); (3) the National Centers for Environmental Prediction/National Center for Atmospheric Research (NCEP/NCAR) reanalysis data from 1958 to 2001 (Kalnay et al., 1996); and (4) observational SST data obtained from the Global Sea-Ice and Sea Surface Temperature (GISST) dataset (Rayner et al., 2003).

In addition to observational data, two sets of model output are used. The first is the global SST-forced ensemble simulation of National Center for Atmospheric Research CAM2.0.1 model (hereafter CAM2) (<http://www.cesm.ucar.edu/models/ccsm2.0.1/cam/camUsersGuide/>). Fifteen runs were carried out using CAM2 and observed SST from January 1949 to October 2001 ([http://www.cesm.ucar.edu/working\\_groups/Variability/index.html](http://www.cesm.ucar.edu/working_groups/Variability/index.html)). Output of the ensemble simulation has already been used in many studies, e.g., the forcing of El Niño upon the Southern Annular Mode (Zhou and Yu, 2004), the remote forcing of sea surface temperature near the maritime continent and equatorial central-eastern Pacific on the inter-annual and inter-decadal variability of the summertime western Pacific subtropical high (Wu and Zhou, 2008), the dominance of the warming trend over the central-eastern Pacific and the western tropical Indian Ocean on the decreasing tendency of global land monsoon precipitation in the past half century (Zhou et al., 2008a), and the predictability of Asian-Australian monsoon circulations (Zhou et al., 2008b). The second model output data source is the 20th century climate simulation of CCSM3 (Collins et al., 2006), which has been conducted for the IPCC AR4 under the leadership of the Joint Scientific Committee/Climate Variability and Predictability of the World Climate Research Programme (WCRP) Working Group on Coupled Modeling (WGCM). The simulation was made with various combinations of forcing agents including greenhouse gases (GHGs), sulfate aerosols, as well as volcanic aerosols and solar variability. Time-varying tropospheric and stratospheric ozone forcing has also been included during the model simulation. The CCSM3 model has reasonable performance in reproducing the 20th century surface air temperature evolution, based on an evaluation by Zhou and Yu

(2006).

The statistical methods used in this study include correlation analysis, regression analysis, power spectra analysis, and Empirical Orthogonal Function (EOF) analysis method. The student's  $t$ -test,  $F$ -test, and Mann-Kendall rank statistics (Sneyers, 1990) were used to test the significance of linear trends.

### 3. Results

#### 3.1 *The leading mode of tropospheric temperature variability in reanalysis*

Previous studies have found that the “South China flood and North China drought” rainfall pattern associated with the inter-decadal scale climate transition occurred by the end of 1970s is most significant in July and August (JA), and the inter-decadal scale tropospheric cooling over East Asia is also significant in JA (Yu et al., 2004b; Yu and Zhou, 2007). Hence, the analyses presented below mainly focus on the JA mean conditions. We begin our study on the harmonious changes of July–August upper tropospheric temperature across the North Atlantic, Eurasian continent, and North Pacific by analyzing the long-term trends. The linear trends are estimated as the slope of a straight line fitted (in a least squares sense) to the observed anomalous troposphere temperature data at each grid point, based on the reference periods defined. Figure 1a shows the linear trends in the JA mean upper troposphere temperature (250–300 hPa slab-averaged) across the entire 44 years. The prominent features include a significant cooling center located over East Asia and two warming centers located over the North Atlantic and the North Pacific. The amplitude of the cooling center over East Asia is  $0.5 \text{ K (10 yr)}^{-1}$ . The amplitude of the warming center over the North Atlantic (North Pacific) is  $0.4 \text{ K (10 yr)}^{-1}$  [ $0.3 \text{ K (10 yr)}^{-1}$ ]. The cooling is far stronger than the warming in strength. The center over East Asia resembles that shown in Yu et al. (2004b). It should be noted that the cooling and warming anomalies are significant from 500 hPa to 200 hPa, reaching a maximum at 250–300 hPa. To highlight the anomalies, we confine the core analyzed levels to 250–300 hPa in this study.

Since the linear trend does not definitively indicate inter-decadal scale variations, we further explore the coherent variation of tropospheric temperature change across Northern Hemisphere by performing EOF analysis upon the JA mean temperature anomalies. Figure 1b shows the spatial pattern of the first leading EOF mode of the 250–300 hPa slab-averaged temperature anomalies, which is obtained by analysis of the cor-

relation matrix based on the ERA40 data set. The fractional variance of the first leading EOF mode is 22.2%. The EOF2 mode (pattern not shown) accounts for 13.2% of the total variance. According to the rule of North et al. (1982), the observed first two leading modes are well distinguished from each other in terms of the sampling error bars, and hence are statistically significant. A same analysis based on the NCEP/NCAR reanalysis shows similar features, indicating the dataset-independence of the result of EOF analysis (figure not shown). Given the resemblance of the trends of the EOF1 modes, we focus our discussion on the first leading mode here. The first leading mode reflects a zonal land-sea asymmetry pattern, which is dominated by three anomalous centers located over the North Atlantic, East Asia, and the North Pacific, respectively. This distribution closely resembles Fig. 1a except with a reversed sign, having a pattern correlation coefficient of  $-0.75$ . The pattern correlation coefficient is calculated as temporal correlation but uses data at all gridpoints instead of time samples. The corresponding principal component (hereafter PC1) is given in Fig. 1c, which shows a decreasing tendency for the entire period examined, particularly before 1980. The linear trend of the PC is  $-2.5 (50 \text{ yr})^{-1}$ , which is significantly different from zero at the 1% confidence level based on Mann-Kendall rank statistics. Note that before performing EOF analysis, the zonal mean condition has been subtracted from the raw data. If we directly perform EOF analysis on the raw data, the EOF1 mode presented above appears as the EOF2 mode, and the explained variance is nearly the same (figures not shown).

The leading mode of Northern Hemisphere tropospheric temperature change is featured by the three anomalous centers located over the North Atlantic, East Asia, and the North Pacific, respectively. To exhibit evolutions of the upper tropospheric temperature over the above three target domains, the time series of JA 250–300 hPa mean anomalous temperature averaged respectively over three core areas (i.e., the central shaded areas over the North Atlantic, East Asia, and North Pacific shown in Fig. 1b) are presented in Fig. 2. Both the North Atlantic and the North Pacific show warming trends in the upper troposphere, particularly before the late 1980s. The warming trend over the North Pacific is more significant before the late 1970s. In fact, after the late 1980s, there appears to be a slightly decreasing tendency. The warming trend over the North Atlantic has also leveled off since the mid-1980s. In contrary to the conditions of the North Atlantic and North Pacific, the upper troposphere over East Asia exhibits a robust cooling trend, particularly before the 1980s, as evidenced in Yu et al. (2004b).

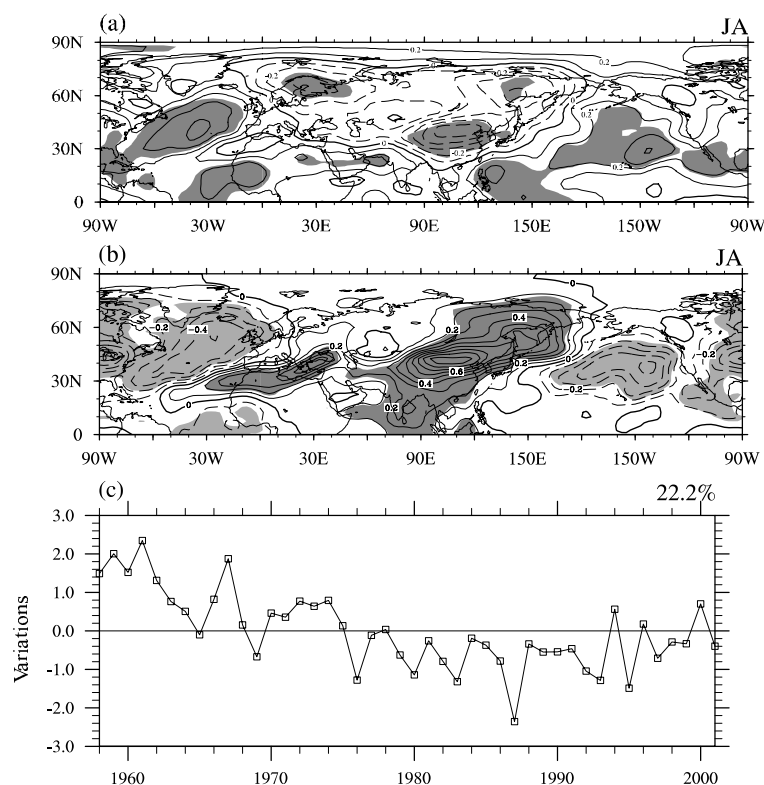


**Fig. 1.** (a) Trends of JA slab-averaged temperature anomalies between 250 hPa and 300 hPa, units:  $\text{K} (10 \text{ yr})^{-1}$ . Areas exceeding a confidence level of 95% using an  $F$ -test are shaded. (b) Spatial pattern of the leading Empirical Orthogonal Function (EOF) mode of the JA 250–300 hPa slab-averaged temperature and (c) the corresponding principle component (unitless). The air temperature data come from the ERA-40 and the zonal mean condition has been subtracted before performing EOF analysis. The EOF pattern of (b) is shown as the temperature anomalies regressed upon the associated PC (unitless). The shadings outline the regions exceeding a confidence level of 99% using student's  $t$ -test.

The variation is relatively stable after the 1980s and has no significant trend. Hence, there appears to be a harmonious change of the upper tropospheric temperature across the mid-latitudes (30–60 N) for the North Atlantic, the Eurasian continent, and the North Pacific. This harmony is further demonstrated by the significant correlations among the indices, as shown in Table 1. While the North Atlantic and the North Pacific are positively correlated with each other in the defined indices, having a correlation coefficient of 0.59, which is statistically significant at the 5% level, both of them have significant negative correlations (i.e.,  $-0.80$  and  $-0.77$ , both statistically significant at the 0.05 level) with East Asia in the upper tropospheric temperature variations. After removing the linear trends, the corresponding correlation coefficients decrease slightly, but are still nearly significant at the 0.05 level by using student's  $t$ -test.

### 3.2 The tropospheric temperature variation in radiosonde data

The analyses outlined above are based on the 250–300 hPa data in reanalysis. Visual inspections of Figs. 1–2 show that there are some transition or jump points. For example, a conspicuous jump is evident in 1968/69 in Figs. 1c and 2a, and weaker jumps are also visible in Figs. 2b–c. Since the 250 hPa level became a standard pressure level in the late 1960s and most radiosonde stations did not report at this level before 1968, it is possible that the introduction of these data has introduced a spurious jump-like signal in the reanalysis, which depends only on radiosonde data at high levels. To confirm that the results found here are not based on spurious signals in the reanalysis, and also to reduce uncertainties relevant to the quality of reanalysis data, the time series of 250–300 hPa mean temperature averaged over the three target domains is













